

## Polynuclear Ag(I)-*N*-heterocyclic carbene complexes: synthesis, electrochemical and *in vitro* anticancer study against human breast cancer and colon cancer

Aqsa Habib, Muhammad Adnan Iqbal & Haq Nawaz Bhatti

To cite this article: Aqsa Habib, Muhammad Adnan Iqbal & Haq Nawaz Bhatti (2019): Polynuclear Ag(I)-*N*-heterocyclic carbene complexes: synthesis, electrochemical and *in vitro* anticancer study against human breast cancer and colon cancer, Journal of Coordination Chemistry, DOI: [10.1080/00958972.2019.1632837](https://doi.org/10.1080/00958972.2019.1632837)

To link to this article: <https://doi.org/10.1080/00958972.2019.1632837>

 View supplementary material 

 Published online: 02 Jul 2019.

 Submit your article to this journal 

 View Crossmark data 



# Polynuclear Ag(I)-*N*-heterocyclic carbene complexes: synthesis, electrochemical and *in vitro* anticancer study against human breast cancer and colon cancer

Aqsa Habib, Muhammad Adnan Iqbal and Haq Nawaz Bhatti

Department of Chemistry, University of Agriculture Faisalabad, Punjab, Pakistan

## ABSTRACT

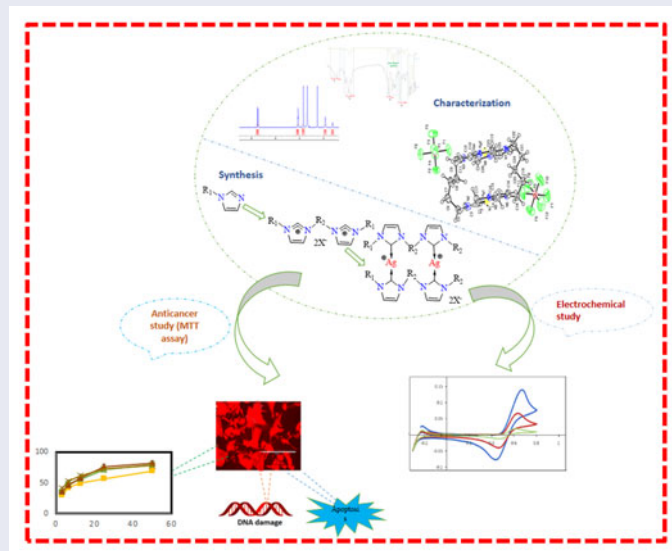
Four new bis-imidazolium salts **3–6** and their di- and polynuclear silver(I)-*N*-heterocyclic carbene (Ag(I)-NHC) complexes **7–10** were synthesized and characterized by using various analytical techniques. Single-crystal studies of **8** revealed a dinuclear structure whereas that of **9** revealed an interesting polynuclear structure. The quasi-reversibility of redox events in electrochemical study of **9** indicated that reduction produces unstable decomposed species and oxidation may be ascribed to these decomposed species. All the compounds were studied for their *in vitro* anticancer study against human breast cancer (MDA-MB-231) and colon cancer (HCT-116) cells. The study revealed that Ag(I)-NHC complexes are comparatively more potent than NHC precursors (salts). MDA-MB-231 cells appeared more sensitive to complexes than HCT-116 cells while reverse is the case for NHC salts.

## ARTICLE HISTORY

Received 8 February 2019  
Accepted 1 June 2019

## KEYWORDS

Polymeric; quasi-reversible; redox process; HCT-116



## 1. Introduction

Ag(I)–*N*-heterocyclic carbene complexes (Ag(I)–NHCs) are moisture and air stable class of compounds which can be easily synthesized by simple reported protocols including (1) the reaction of free carbenes with suitable sources of silver, (2) the reaction of silver sources with azolium salts in alkaline medium to generate alkaline phase-transfer conditions and (3) the reaction of basic silver sources with azolium salts [1–3].

The striking features of NHC ligands make them suitable for the formation of metal-based polymeric frameworks which is still least studied area [4]. Polydentate-NHC ligands, on the account of their chelating or pincer effects, have become the pronounced species to target mixed-valence, polymeric or high-oxidation state complexes by producing stable metal–ligand system with a variety of coordination spheres and remarkable chemical and medicinal features [5–7]. Polymeric silver(I)–NHC systems with aliphatic or aromatic moieties as linkers have become a novel class of silver-based drugs with pronounced anticancer potential on the account of their biocompatibility [8] but only few examples of silver-based multinuclear/supramolecular coordination motifs having weak Ag–Ag interactions (3.1–3.4 Å) or metal–carbon/metal–heteroatom interactions have been reported [9].

Breast cancer is the most substantial sort of human non-skin malignancy and the second major cause of women mortality in western countries, while human colon cancer is among the most common types of cancer and major cause of deaths all over the world [10, 11]. Numerous silver-based drugs are already in the market for treatment of both cancer types, but almost all have several side effects including allergy, fatigue, seizures, bleeding, thrombocytopenia, renal damage, alopecia, peripheral neuropathy, blood dyscrasias, hepatotoxicity and nephrotoxicity, destruction of central nervous system and oligodendrocytes [12]. The major cause of these side-effects is the fast release of Ag<sup>+</sup> ions which in turn destroys the normal cells in addition to diseased cells during their activity [13]. The disadvantages of these market drugs have attracted the attention of researchers to introduce new metallodrugs having little or no side-effects [14–21]. Recently, gold- and silver(I)–NHC complexes have been examined for their anticancer potential against human breast cancer and colon cancer cell lines [22, 23]. Ag(I)–NHC complexes are surpassing some already available market silver-based drugs [24]. The complexes bearing various substituents have been observed to pose strong biopotential due to sustained release of Ag<sup>+</sup> ions which depends on their electronic and steric features influencing their lipophilicity [25].

In previous studies, we have explored the anticancer potential of substituted benzimidazolium-based silver complexes [2, 3]. This manuscript describes augmentation of the previous studies. We report the synthesis of three dinuclear and one unique polymeric Ag(I)–NHC complex. To best of our knowledge, such a polymeric structure without silver–silver bonding as we document for **9** has not yet been reported. We have afforded these complexes from bis-imidazolium based NHC ligands and studied their electrochemical and anticancer properties.

## 2. Materials and methods

### 2.1. Chemicals

Imidazole, 1-methyl imidazole, alkyl halides (1,5-dibromopentane, bromodiphenylmethane, 1,3-bis(bromomethyl)benzene, 1,4-bis(bromomethyl)benzene, 1,4-dibromobutane)

and Ag<sub>2</sub>O were purchased from Sigma Aldrich. Phosphate buffered saline (PBS), penicillin/streptomycin solution (PS), 5-fluorouracil and 3-(4,5-dimethylthiazol-2-yl)-2,5-diphenyl-tetrazolium bromide (MTT) reagent were purchased from Sigma-Aldrich. Human colon cancer (HCT-116) and breast cancer (MDA-MB-231) cells were obtained from the American type culture collection (Rockville, MD, USA).

## 2.2. Instrumentation

The melting points of the synthesized compounds were evaluated with the help of a Stuart Scientific SMP-1 (UK) instrument. Low-boiling point solvents were removed by an EYELA 1L Rotary Evaporator N-1001V-WD. To monitor the alkylation reactions, Agilent Technologies 7890A GC/MS (Gas chromatography/Mass spectrometry) was used. The FTIR (Fourier transform infrared spectroscopy) spectra were obtained with an ALPHA-P, compact FTIR spectrometer. <sup>1</sup>H, <sup>13</sup>C, <sup>31</sup>P and <sup>19</sup>F NMR spectra were taken on a Bruker Avance-300 and Avance-400 or on a Varian Inova-300 spectrometer in deuterated solvents. Chemical shifts are given in ppm while *J* values are given in Hertz. Spectral assignments were achieved by <sup>1</sup>H–<sup>13</sup>C HSQC (Heteronuclear single quantum coherence) experiments. The elemental analysis of the synthesized compounds was carried out by 180508E; Fisons Instruments EA 1108 CHNS analyzer. The crystallographic data for **8** and **9** were collected on a Bruker APEX II as reported [2, 3]. The electrochemical measurements were performed to investigate the redox properties of compounds by testing their reactivity toward chemical oxidant using a BASI-Epsilon potentiostat, at a scan rate of 100 mV s<sup>-1</sup> under N<sub>2</sub> at room temperature. Tetrabutyl ammonium hexafluoro phosphate [nBu<sub>4</sub>N][PF<sub>6</sub>] (1 mM in CH<sub>3</sub>CN) was used as a supporting electrolyte and the sample was 1 mM. Ag/AgCl was used as reference, platinum disk as working and platinum wire as counter electrodes. For calibration, ferrocene (1 mmol) was added as an internal standard. IC<sub>50</sub> values were determined with a TECAN Multi-mode microplate reader obtained from USA.

## 2.3. Synthesis of pre-ligands (1 and 2)

### 2.3.1. Methyl imidazole (1)

Compound **1** was purchased from Sigma Aldrich.

### 2.3.2. 1-Benzhydryl 1H-imidazole (2)

A mixture of imidazole (0.68 g, 10 mmol), bromodiphenylmethane (2.47 g, 10 mmol) and KOH (0.84 g, 15 mmol) in DMSO (20 mL) was stirred at room temperature until the reaction was complete (as monitored by GC-MS). To remove DMSO (Dimethyl Sulfoxide), the mixture was poured in cold distilled water (200 mL) and extracted the product with a mixture of ether and hexane (25 mL, 1:1) and washed it with cold water. The product contained in organic layer was isolated and purified by adding MgSO<sub>4</sub> to remove residual water. After solvent removal, oily product was obtained. Yield 1.52 g (65%). GC-MS, *m/z*, (%): ([C<sub>16</sub>H<sub>14</sub>N<sub>2</sub>]<sup>+</sup> 234.3 (100). FTIR (cm<sup>-1</sup>): 2958, 2872 (C<sub>aliph</sub>-H str), 1494, 1457, 1364 (C[dbond]N<sub>imid</sub> str), 1285, 1259, 1150 (C<sub>arom</sub>-N<sub>imid</sub> str), 841, 738, 632 (C<sub>arom</sub>-H<sub>imid</sub> ben). <sup>1</sup>H NMR (400 MHz, CDCl<sub>3</sub>), δ (ppm): 6.26 (1H, s, 1 × CH),

6.86 (1H, d,  $H_{\text{imid}}$ ,  $J = 7.53$  Hz), 7.23 (4H, d,  $H_{\text{imid}}$ ,  $J = 7.5$  Hz), 7.26 (1H, d,  $H_{\text{imid}}$ ,  $J = 7.81$  Hz), 7.33 (4H, t,  $H_{\text{imid}}$ ,  $J = 7.3$  Hz), 7.96 (1H, N-CH- $N_{\text{imid}}$ ). Anal. Calcd for  $C_{16}H_{14}N_2$  (%): C, 80.02; H, 6.02; N, 11.96. Found C, 80.61; H, 6.31; N, 11.56.

## 2.4. Synthesis of ligands (3–6)

### 2.4.1. 1-Methyl-3-(4-(3-methyl-1H-imidazol-3-ium-1-yl) butyl)-1H-imidazol-3-ium bromide (3)

A mixture of **1** (1.6 mL, 20 mmol) and 1,4-dibromobutane (6 mL, 50 mmol, excess) was refluxed at 120 °C for 48 h and monitored the reaction by GC-MS. Upon completion of reaction, oily layer settled down, decanted, washed the residue with ether (3 × 3 mL) and dried at 40 °C. Compound **3** was formed as white powder. Yield 1.5 g (75%); m.p. 113–115 °C. FTIR ( $\text{cm}^{-1}$ ): 2936, 2873 ( $C_{\text{aliph-H}}$  str), 1566, 1456, 1400, 1363 ( $C[\text{dbond}]N_{\text{imid}}$  str), 1163 ( $C_{\text{arom-Nimid}}$  str), 823, 788, 744, 623 (C- $H_{\text{imid}}$  ben).  $^1\text{H}$  NMR (400 MHz,  $\text{CDCl}_3$ ),  $\delta$  (ppm): 1.76 (4H, t,  $\text{CH}_2$ ,  $J = 3.02$  Hz), 3.83 (6H, s,  $2 \times \text{CH}_3$ ), 4.21 (4H, s,  $2 \times \text{R-CH}_2\text{-N}$ ,  $J = 6.65$  Hz), 7.73 (4H, d.t,  $H_{\text{imid}}$ ,  $J = 7.92$  Hz), 9.11 (2H, s, N-CH-N).  $^{13}\text{C}$  NMR (125.72 MHz,  $\text{CDCl}_3$ ),  $\delta$  (ppm): 26.5 ( $\text{CH}_3\text{-N}$ ), 36.2 (R- $\text{CH}_2\text{-R}$ ), 48.4 (R- $\text{CH}_2\text{-N}$ ), 122.6, 124.2 ( $C_{\text{imid}}$ ), 137.0 (N[ $\text{dbond}$ ]C[ $\text{dbond}$ ]N).  $^{19}\text{F}$  (470.4 MHz,  $\text{CDCl}_3$ ),  $\delta$  (ppm): -72.2 (d, 6F).  $^{31}\text{P}$  (202.4 MHz,  $\text{CDCl}_3$ ),  $\delta$  (ppm): -145.1 (h, 1P). Anal. Calcd for  $C_{12}H_{20}N_4Br_2$  (%): C, 37.92; H, 5.30; N, 14.74. Found C, 37.21; H, 5.12; N, 14.87.

### 2.4.2. 1-Methyl-3-(5-(3-methyl-1H-imidazol-3-ium-1-pentyl)-1H-imidazol-3-ium bromide (4)

The same procedure for formation of **3** was followed to synthesize **4** using 1,5-dibromopentane (4 mL, 29.3 mmol, excess). After work up, **4** was obtained as white powder. Yield 2.16 g (55%); m.p. 120–122 °C. FTIR ( $\text{cm}^{-1}$ ): 3420 ( $C_{\text{aliph-Nimid}}$ ), 2935, 2862 ( $C_{\text{aliph-H}}$  str), 1576, 1561, 1463, 1384, 1365 ( $C[\text{dbond}]N_{\text{imid}}$  str), 1184 ( $C_{\text{arom-Nimid}}$ ), 875, 840, 771, 756, 621 (C- $H_{\text{imid}}$  ben).  $^1\text{H}$  NMR (400 MHz,  $\text{CDCl}_3$ ),  $\delta$  (ppm): 1.63 (2H, m,  $\text{CH}_2$ ), 2.11 (4H, m,  $2 \times \text{CH}_2$ ), 4.12 (6H, s,  $2 \times \text{CH}_3$ ), 4.50 (4H, t, R- $\text{CH}_2\text{-N}$ ), 7.24 (2H, s,  $H_{\text{imid}}$ ), 7.81 (2H, s,  $H_{\text{imid}}$ ), 10.50 (2H, s, N-CH-N).  $^{13}\text{C}$  NMR (125.72 MHz,  $\text{CDCl}_3$ ),  $\delta$  (ppm): 28.9 ( $\text{CH}_2$ ), 30.9 ( $\text{CH}_2$ ), 36.8 ( $\text{CH}_2$ ), 49.2 ( $\text{CH}_3\text{-N}$ ), 65.8 ( $\text{CH}_2\text{-N}$ ), 122.8 ( $N_{\text{imid}}[\text{dbond}]C[\text{dbond}]N_{\text{imid}}$ ). Anal. Calcd for  $C_{13}H_{22}N_4Br_2$  (%): C, 39.61; H, 5.63; N, 14.21. Found C, 39.21; H, 5.69; N, 14.99.

### 2.4.3. 1-Methyl-3-(3-((3-methyl-1H-imidazole-3-ium-1-methyl) benzyl)-1H-imidazol-3-ium chloride (5)

The same procedure for formation of **3** was followed to synthesize **5** using 1,3-bis(bromomethyl)benzene (1.75 g, 10 mmol). After work up, **5** was obtained as white powder. Yield 2.4 g (72%); m.p. 170 °C. FTIR ( $\text{cm}^{-1}$ ): 3365 ( $C_{\text{aliph-Nimid}}$ ), 2983, 2870 ( $C_{\text{aliph-H}}$  str), 1563, 1455 ( $C[\text{dbond}]N_{\text{imid}}$  str), 1172 ( $C_{\text{arom-Nimid}}$ ), 809, 789, 754, 623 (C- $H_{\text{imid}}$  ben).  $^1\text{H}$  NMR (400 MHz,  $\text{CDCl}_3$ ),  $\delta$  (ppm): 3.87 (6H, s,  $2 \times \text{CH}_3$ ), 5.42 (4H, s,  $2 \times \text{CH}_2$ ), 7.39 (2H, d,  $H_{\text{imid}}$ ,  $J = 7.29$  Hz), 7.48 (2H, m,  $H_{\text{imid}}$ ), 7.74 (4H, s,  $H_{\text{imid}}$ ), 9.21 (2H, s, N-CH-N).  $^{13}\text{C}$  NMR (125.72 MHz,  $\text{CDCl}_3$ ),  $\delta$  (ppm): 35.9 ( $\text{CH}_3$ ), 51.53 ( $\text{CH}_2$ ), 122.4, 124.1, 128.6, 128.7, 129.7, 135.7 (Ar-C), 136.9 (N[ $\text{dbond}$ ]C[ $\text{dbond}$ ]N). Anal. Calcd for  $C_{16}H_{20}N_4Cl_2$ (%): C, 56.64; H, 5.94; N, 16.51. Found C, 56.21; H, 5.69; N, 16.99.

#### 2.4.4. 1-Benzhydryl-3-(4-(3-benzhydryl-1H-imidazol-3-ium-1-methyl)benzyl)-1H-imidazol-3-ium bromide (6)

The same procedure for formation of **3** was followed to synthesize **6** using **2** (1.15 mL, 5 mmol) and 1,4-bis(bromomethyl)benzene (0.66 g, 2.5 mmol). After work up, **6** was obtained as white powder. Yield 1.19 g (65%); m.p. 120–125 °C. FTIR (cm<sup>-1</sup>): 2987 (C<sub>aliph</sub>-H str), 1543, 1448, 1418 (C[dbond]N<sub>imid</sub> str), 1189, 1008 (C<sub>arom</sub>-N<sub>imid</sub> str), 754.8, 702.6 (C-H<sub>imid</sub> ben). <sup>1</sup>H NMR (400 MHz, CDCl<sub>3</sub>), δ (ppm): 3.56 (4H, s, N-CH<sub>2</sub>-Ar), 5.81 (2H, s, Ph<sub>2</sub>-CH-N), 7.52 (14H, m, Ar-H), 7.80 (8H, d, Ar-H, *J* = 7.31 Hz), 9.71 (2H, s, N-CH-N). <sup>13</sup>C NMR (125.72 MHz, CDCl<sub>3</sub>), δ (ppm): 50.2 (Ar-CH<sub>2</sub>-N), 64.7 (Ph<sub>2</sub>-CH-N), 127.3, 127.4, 128.93, 129.8, 131.8, 134.9 (Ar-C), 136.5 (Ph<sub>2</sub>-CH-N), 142.8 (N[dbond]C[dbond]N<sub>imid</sub>). Anal. Calcd for C<sub>40</sub>H<sub>36</sub>N<sub>4</sub>Br<sub>2</sub>(%): C, 65.58; H, 4.95; N, 7.65. Found C, 65.65; H, 4.69; N, 7.69.

### 2.5. Synthesis of Ag(I)-NHC complexes (7–10)

#### 2.5.1. Bis(1-methyl-3-(5-(3-methyl-1H-imidazol-3-ium-1-butyl)-1H-imidazol-3-ium silver) bis(hexafluorophosphate) (7)

A mixture of **3** (2.6 g, 7 mmol) and silver oxide (3.5 g, 14 mmol) in methanol (120 mL) was stirred for 48 h at room temperature in complete darkness. After filtration of black suspension, aqueous solution of potassium hexafluorophosphate (2.54 g, 14 mmol) was added to exchange the counterions as the complex with halide counterions was highly photosensitive/unstable in solution form and decomposed during isolation attempts. The mixture was allowed to stir for 4 h at room temperature. The precipitates obtained were filtered and dried at room temperature. Compound **7** was obtained as beige powder. Yield 3.8 g (62%); m.p. 240–242 °C. FTIR (cm<sup>-1</sup>): 2857, (C<sub>aliph</sub>-H str), 1523, 1414, 1401, 1313 (C[dbond]N<sub>imid</sub> str), 821, 718 (C-H<sub>imid</sub> ben). <sup>1</sup>H NMR (400 MHz, DMSO-d<sub>6</sub>), δ (ppm): 1.91 (8H, m, 4 × CH<sub>2</sub>), 3.69 (12H, s, 4 × CH<sub>3</sub>), 4.31 (8H, t, 4 × R-CH<sub>2</sub>-N, *J* = 6.75 Hz), 7.50 (8H, s, Ar-H). <sup>13</sup>C NMR (125.72 MHz, DMSO-d<sub>6</sub>), δ (ppm): 31.0 (CH<sub>2</sub>), 38.3 (CH<sub>2</sub>), 51.7 (CH<sub>3</sub>-N), 122.1, 123.8 (C<sub>imid</sub>), 179.2, 180.7 (d, Ag-C-Ag, *J* = 190.6 Hz). <sup>19</sup>F (470.4 MHz, DMSO-d<sub>6</sub>), δ (ppm) -72.5 (d, 6F). <sup>31</sup>P (202.4 MHz, DMSO-d<sub>6</sub>), δ (ppm) -144.3 (h, 1P). Anal. Calcd for C<sub>24</sub>H<sub>36</sub>Ag<sub>2</sub>F<sub>12</sub>N<sub>8</sub>P<sub>2</sub> (%): C, 30.59; H, 3.85; N, 11.89. Found C, 31.10; H, 3.90; N, 11.56.

#### 2.5.2. Bis(1-methyl-3-(5-(3-methyl-1H-imidazol-3-ium-1-pentyl)-1H-imidazol-3-ium silver) bis(hexafluorophosphate) (8)

The same procedure for the formation of **7** was followed to synthesize **8** using **4** (2.7 g, 7 mmol). Compound **8** was obtained as beige powder. Yield 3.5 g (57%); m.p. 240 °C. FTIR (cm<sup>-1</sup>): 2957, 2872 (C<sub>aliph</sub>-H str), 1567, 1457, 1404, 1398 (C[dbond]N<sub>imid</sub> str), 862, 740 (C-H<sub>imid</sub> ben). <sup>1</sup>H NMR (400 MHz, DMSO-d<sub>6</sub>), δ (ppm): 1.21 (4H, m, CH<sub>2</sub>), 1.85 (8H, m, 2 × CH<sub>2</sub>), 3.67 (6H, s, 2 × CH<sub>3</sub>), 4.11 (8H, t, R-CH<sub>2</sub>-N, *J* = 6.79 Hz), 7.42 (4H, s, Ar-H), 7.50 (4H, s, Ar-H). <sup>13</sup>C NMR (125.72 MHz, DMSO-d<sub>6</sub>), δ (ppm): 23.6 (CH<sub>2</sub>), 31.0 (CH<sub>2</sub>), 38.2 (CH<sub>2</sub>), 51.5 (CH<sub>3</sub>-N), 122.2, 123.5 (C<sub>imid</sub>), 179.0, 180.9 (d, Ag-C-Ag, *J* = 190.6 Hz). <sup>19</sup>F (470.4 MHz, DMSO-d<sub>6</sub>), δ (ppm): -72.5 (d, 6F). <sup>31</sup>P (202.4 MHz, DMSO-d<sub>6</sub>), δ (ppm): -144.3 (h, 1P). Anal. Calcd for C<sub>26</sub>H<sub>40</sub>Ag<sub>2</sub>F<sub>12</sub>N<sub>8</sub>P<sub>2</sub> (%): C, 32.18; H, 4.16; N, 11.55. Found C, 32.18; H, 4.15; N, 11.41.

### 2.5.3. *Bis(1-methyl-3-(3-((3-methyl-1H-imidazole-3-ium-1-methyl)benzene)-1H-imidazol-3-ium silver) bis(hexafluorophosphate) (9)*

The same procedure for the formation of **7** was followed to synthesize **9** using **5** (2.3 g, 7 mmol). Compound **9** was obtained as beige powder. Yield 2.4 g (53%); m.p. 175–180 °C. FTIR (cm<sup>-1</sup>): 2936, 2873 (C<sub>aliph</sub>-H str), 1566, 1460, 1400, 1360 (C[dbond]N<sub>imid</sub> str), 827, 742 (C-H<sub>imid</sub> ben). <sup>1</sup>H NMR (400 MHz, DMSO-d<sub>6</sub>), δ (ppm): 3.67 (12H, s, 4 × CH<sub>3</sub>), 5.21 (8H, s, 4 × CH<sub>2</sub>), 7.12 (6H, d, Ar-H, *J* = 37.58 Hz), 7.31 (2H, m, Ar-H), 7.49 (8H, d, Ar-H, *J* = 16.55 Hz). <sup>13</sup>C NMR (125.72 MHz, DMSO-d<sub>6</sub>), δ (ppm): 31.1 (CH<sub>3</sub>), 54.0 (CH<sub>2</sub>), 118.5 (N-CH<sub>imid</sub>), 125.9, 127.2, 129.7, 138.3 (Ar-C), 179.9, 181.8 (s, N[dbond]C[dbond]N, *J* = 190.5 Hz). <sup>19</sup>F (470.4 MHz, DMSO-d<sub>6</sub>), δ (ppm): -73.2 (d, 6F). <sup>31</sup>P (202.4 MHz, DMSO-d<sub>6</sub>, δ ppm) -144.2 (h, 1P). Anal. Calcd for C<sub>32</sub>H<sub>36</sub>Ag<sub>2</sub>F<sub>12</sub>N<sub>8</sub>P<sub>2</sub> (%): C, 37.01; H, 3.49; N, 10.79. Found C, 37.12; H, 3.51; N, 10.85.

### 2.5.4. *Bis(1-benzhydryl-3-(4-((3-benzhydryl-1H-imidazol-3-ium-1-methyl) benzene)-1H-imidazol-3-ium silver) bis(hexafluorophosphate) (10)*

The same procedure for the formation of **7** was followed to synthesize **10** using **6** (2.1 g, 3 mmol) and silver oxide (1.6 g, 6 mmol). Complex **10** was obtained as beige powder. Yield 1.1 g (55%); m.p. 120–125 °C. FTIR (cm<sup>-1</sup>): 2905 (C<sub>aliph</sub>-H str), 1492, 1448 (C[dbond]N<sub>imid</sub> str), 1183, 1259, 1049 (C<sub>arom</sub>-N<sub>imid</sub> str), 772, 738 (C-H<sub>imid</sub> ben). <sup>1</sup>H NMR (400 MHz, DMSO-d<sub>6</sub>), δ (ppm): 3.52 (8H, s, N-CH<sub>2</sub>-Ar), 5.41 (4H, s, Ph<sub>2</sub>-CH-N), 7.21 (8H, t, Ar-H, *J* = 7.3 Hz), 7.33 (24H, t, Ar-H, *J* = 7.7 Hz), 7.377 (16H, d, 7.33 Hz). <sup>13</sup>C NMR (125.72 MHz, DMSO-d<sub>6</sub>), δ (ppm): 49.1 (Ar-CH<sub>2</sub>-N), 63.2 (Ph<sub>2</sub>-CH-N), 127.1, 127.8, 128.9, 133.1, 137.4 (Ar-C), 142.6 (Ph<sub>2</sub>-CH-N), 193.2, 196.3 (s, C-Ag-C). <sup>19</sup>F (470.4 MHz, DMSO-d<sub>6</sub>), δ (ppm): -72.6 (d, 6F). <sup>31</sup>P (202.4 MHz, DMSO-d<sub>6</sub>), δ (ppm): -143.8 (h, 1P). Anal. Calcd for C<sub>80</sub>H<sub>68</sub>Ag<sub>2</sub>F<sub>12</sub>N<sub>8</sub>P<sub>2</sub> (%): C, 58.34; H, 4.16; N, 6.8. Found C, 57.99; H, 4.56; N, 7.1.

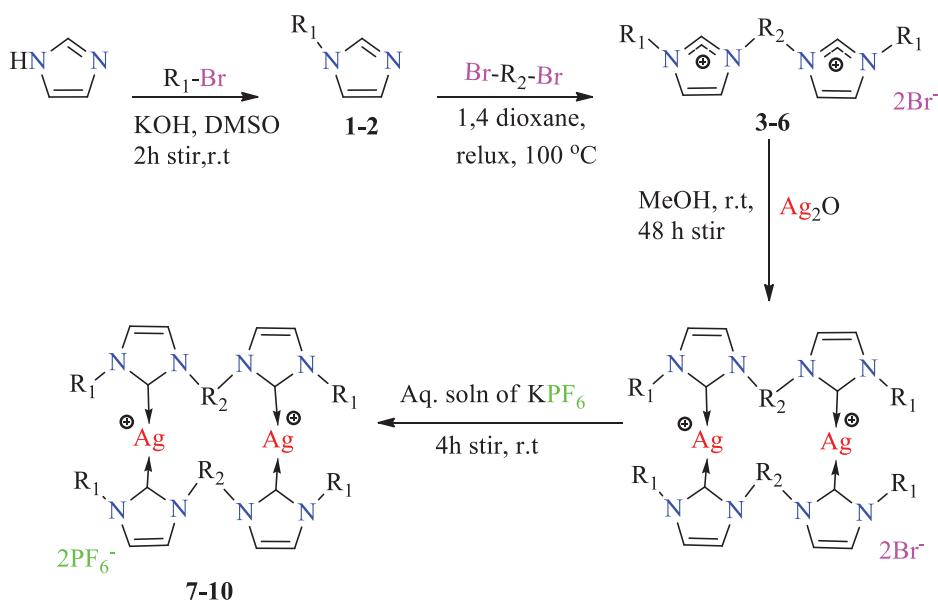
MTT assay was performed according to reported method [2, 3].

## 3. Results and discussion

The syntheses of the NHC precursors and their silver complexes were successfully achieved by following our reported protocol [2, 13, 22]. The complexes with halide counterions are highly photosensitive/unstable in solution form and usually decompose during isolation attempts, so as to get stable end product, the counterions were exchanged *in situ* with hexafluorophosphate ions by adding two equivalent aqueous solution of KPF<sub>6</sub> after metallation step. Scheme 1 shows the simple steps of the syntheses of precursors and complexes. Fully sketched chemical structures of all the synthesized compounds have been given in the Supplementary data file (Figure S1).

### 3.1. Characterization

The preliminary structural elucidation of the synthesized compounds was obtained from FTIR analysis. Strong vibrational bands appeared at 3402–3424 cm<sup>-1</sup> due to C<sub>aliph</sub>-N<sub>imi</sub> stretching vibrations of the preligands **1** and **2** and ligands **3–6** [8, 13] (Figures S2–S5). C[dbond]N<sub>imidazole</sub> stretching vibrations appeared at 1350–1500 cm<sup>-1</sup> for **1** and **2** and **3–6**, however, in the case of **7–10** these signals were observed in



For compound <b>1</b> :	$R_1 = CH_3-$	-
For compound <b>2</b> :	$R_1 = (C_6H_5)_2-CH-$	-
For compounds <b>3, 7</b> :	$R_1 = CH_3-$	$R_2 = C_4H_8-$
For compounds <b>4, 8</b> :	$R_1 = CH_3-$	$R_2 = C_5H_{10}-$
For compounds <b>5, 9</b> :	$R_1 = CH_3-$	$R_2 = 1,3-(C_2H_4)_2-C_6H_4$
For compounds <b>6, 10</b> :	$R_1 = (C_6H_5)_2-CH-$	$R_2 = 1,4-(C_2H_4)_2-C_6H_4$

**Scheme 1.** Synthesis of *N*-alkylated-imidazoles (**1** and **2**), *N,N'*-dialkylated-imidazolium salts (**3–6**) and Ag(I)-NHC complexes (**7–10**).

specific “four fingers (*f.fs*)” pattern [26] which provided evidence of complex formation [27] (Figures S2–S7).

NMR studies further supported the evidences of synthesis. Ligands **3–6** displayed alkyl group resonances at 6.0–8.0 ppm in  $^1H$  NMR spectra and a signal for the most de-shielded acidic proton and carbon (NCHN) between 9.0 and 12.0 ppm in  $^1H$  NMR and 140 and 150 ppm in  $^{13}C$  NMR spectra, respectively [13] (Figures S8–S14). The progress of the metalation reaction of **3–6** to form silver complexes **7–10** was evident from disappearance of NCHN proton signal (at 9.0–12.0 ppm) which indicated Ag(I)-NHC bonding [28]. This bonding was also confirmed from  $^{13}C$  NMR spectra where these resonances ( $C_{\text{carbene}}-Ag-C_{\text{carbene}}$ ) fall between 180 and 200 ppm [29] in the form of doublet of doublet or in some cases singlets [30]. This behavior is evident in Figures S9–S13 where two singlets appeared in  $^{13}C$  NMR spectra of complexes. Two-dimensional (HSQC)  $^1H$ - $^{13}C$  correlation NMR spectra were helpful to assign signals of  $^1H$  and  $^{13}C$  spectra (Figures S15–S17) [31]. Appearance of septet and doublet in  $^{31}P$  and  $^{19}F$  NMR spectra at  $-141.2$  to  $-144.24$  ppm and  $-71.3$  to  $-72.5$  ppm, respectively, indicated the presence of  $PF_6^-$  counterions with complexes (Figures S18 and S19).

**Table 1.** Crystal data and structure refinement details for **8** and **9**.

Complex	<b>8</b>	<b>9</b>
Formula	C <sub>26</sub> H <sub>40</sub> Ag <sub>2</sub> F <sub>12</sub> N <sub>8</sub> P <sub>2</sub> ·CH <sub>3</sub> CN	C <sub>32</sub> H <sub>36</sub> Ag <sub>2</sub> N <sub>8</sub> F <sub>12</sub> P <sub>2</sub>
Formula weight	1011.39	1038.35
Crystal system	Monoclinic	Triclinic
Space group	<i>P</i> 2 <sub>1</sub> / <i>n</i> (14)	<i>P</i> 1(2)
Unit cell dimensions		
<i>a</i> (Å)	7.5193(11)	8.8761(2)
<i>b</i> (Å)	43.322(6)	11.3841(2)
<i>c</i> (Å)	12.1065(17)	11.3846(2)
$\alpha$ (°)	90	62.8050(10)
$\beta$ (°)	101.872	67.0390(10)
$\gamma$ (°)	90	67.0610(10)
<i>V</i> (Å <sup>3</sup> )	3859.35	910.191
<i>R</i> -factor (%)	–	3.71
<i>Z</i>	4	2
Density (calcd) (g cm <sup>-3</sup> )	1.741	1.894
Abs. coeff. (mm <sup>-1</sup> )	1.190	10.374
<i>F</i> (000)	2024.0	516.0
Crystal size (mm)	0.23 × 0.19 × 0.17	0.1 × 0.07 × 0.03
Temperature (K)	100	100
Radiation (Å)	CuK $\alpha$ 1.54178	CuK $\alpha$ 1.54178
theta Min, max (°)	3.868, 73.046	4.520, 71.692
Data set	–9;9; –53;51; –4;15	–9;10; –14;14; –14;14
Tot.; Uniq. data	7653	9927
<i>R</i> (int)	2842	4059, 3.71
<i>N</i> ref, <i>N</i> par	7762, 483	3565, 325
<i>R</i> , <i>wR</i> 2, <i>S</i>	0.0537 (7423), 0.1416 (7653), 1.043	0.0371 (348), 0.0992 (3464), 1.089

### 3.2. X-ray crystallographic studies

Single-crystals of **8** and **9** were obtained by evaporation of their acetonitrile solution at room temperature. Crystal data are given in Tables 1–3.

X-ray crystal data for **8** indicate that it is a dinuclear compound with molecular formula C<sub>26</sub>H<sub>40</sub>Ag<sub>2</sub>F<sub>12</sub>N<sub>8</sub>P<sub>2</sub>, which crystallizes in monoclinic space group *P*-1(2) having one cationic imidazolium core, two hexafluorophosphate anions and one acetonitrile solvent molecule. Imidazolyl units were found on either side of the central pentyl core. The two NHC moieties attached to one silver center are twisted by 5°. Ag–Ag distances (4.21 Å) are longer than van der Waals radii (3.44 Å) of two silver atoms which is an indication of lack of interaction between Ag–Ag centers of successive dinuclear units [32], hence the molecule which appears as polymer is actually a dinuclear silver complex. Perspective view of **8** is shown in Figure 1.

X-ray crystal data of **9** with molecular formula C<sub>16</sub>H<sub>18</sub>AgN<sub>4</sub>F<sub>6</sub>P indicated that the compound crystallizes in triclinic space group *P*-1(2) having one cationic bis-imidazolium core and two hexafluorophosphate counter anions. The imidazolyl units were found on either side of the central *meta*-xylyl core. The structure appeared as a unique polymer (as shown in Figure 2). Various multinuclear and supramolecular motifs having weak Ag–Ag interactions (3.1–3.4 Å) have been reported [6, 33–35] but according to the best of our knowledge, polymeric structure without silver–silver interaction as we document for **9** is novel in its nature. Perspective view of **9** is shown in Figure 3. The internal imidazole-ring angles (N–C–N) at the carbene center were found between 104.3(4)° to 105.0(4)° in crystal structures of both complexes which are in agreement with the reported values [22]. The bond angle between imidazole ring and pentyl

**Table 2.** Selected bond lengths and angles of **8**.

Bond lengths (Å)		Bond angles (°)		Dihedral angles (°)	
Ag1-C1	2.087(5)	C1-Ag1-C14	176.8(2)	C14-Ag1-C1-N1	84(4)
Ag1-C14	2.081(5)	C10-Ag2-C23	175.4(2)	C1-Ag1-C14-N5	85(4)
Ag2-C23	2.084(5)	C14-N5-C15	111.4(5)	C4-N1-C1-Ag1	-178.5(5)
C3-C10	1.342(7)	C14-N6-C18	124.8(5)	C5-N2-C1-N1	-1.7(8)
C5-C6	1.522(8)	C23-N8-C26	124.5(5)	C5-N2-C1-Ag1	-1.7(8)
C7-C8	1.495(8)	Ag1-C1-N2	129.0(4)	C11-N3-C10-Ag2	178.0(4)
C8-C9	1.572(9)	N1-C1-N2	105.0(4)	C13-N4-C10-Ag2	178.6(5)
C19-C20	1.513(8)	N3-C10-N4	104.8(4)	C6-C7-C8-C9	-163.0(5)

**Table 3.** Selected bond lengths and angles of **9**.

Bond lengths (Å)		Bond angles (°)		Dihedral angles (°)	
Ag1-C13	2.082(3)	C13-Ag1-C2	176.7(2)	C1-N1-C2-Ag1	5.9(7)
N3-C12	1.459(8)	C13-N3-C14	111.1(4)	C2-N2-C4-C3	0.1(6)
N3-C14	1.386(5)	Ag1-C13-N3	128.8(3)	C5-N2-C2-N1	179.4(4)
N4-C15	1.383(5)	Ag1-C13-N4	126.6(3)	C5-N2-C2-Ag1	5.8(7)
C16-C18	1.496(8)	N3-C13-Ag1	128.8(3)	C4-N2-C2-Ag1	175.0(3)
C17-C18	1.41(2)	N4-C13-Ag1	126.6(3)	C2-N1-C3-C4	0.0(6)
C17-C22	1.41(2)	Ag1-C2-N1	128.7(3)	C1-N1-C3-C4	179.4(4)
C18-C19	1.38(1)	Ag1-C2-N2	126.6(3)	C3-N1-C2-Ag1	174.8(4)
C20-C21	1.39(1)	C13-Ag1-C2	176.7(2)	C13-Ag1-C2-N2	46(4)

moiety in **8** was  $125.8(4)^\circ$  for C1-N2-C5 and  $124.7(5)^\circ$  for C22-N7-C23 while between imidazole ring and xylyl moiety of **9** was  $111.6(6)^\circ$  for N4-C16-C18 and  $121.3(6)^\circ$  for N4-C16-C22. N-C and P-F bond distances in both structures were found in the range 1.350(7)–1.47(1) Å and 1.566(4)–1.609(3) Å, respectively. Ag<sup>+</sup> ions were observed in approximately linear coordination geometry between  $175.4(2)^\circ$  and  $176.8(2)^\circ$  for C-Ag-C in both structures. PF<sub>6</sub><sup>-</sup> ions bind to cationic core by feeble electrostatic C...F interaction (3.140 to 6.1 Å) in a 3-D network [8].

### 3.3. Cyclic voltammetry

In cyclic voltammetry experiments, we studied the redox behavior of **8** as a representative and the results are in close agreement with our previous study [3]. The cyclic voltammogram for **8** is shown in Figure 4. As the voltammogram is more drawn out and displays a greater separation in peak potentials (i.e. 400 mV) as compared to a reversible system (separation in peak potentials should be less than 59 mV), the inference could be drawn that a quasi-reversible one-electron redox process (Ag(I)/Ag(0) or Ag(0)/(Ag(I)) is occurring [36]. It can be observed from Figure 4 that during redox cycle, at applied potential in the range of -1.5 to 0 eV, irreversible one-electron redox processes occur at  $E_{1/2}^\circ$  -850 mV (at a scan rate of 100 mV s<sup>-1</sup>). The current is first observed to peak at  $E_{pc}$  -1010 mV (with  $I_{pc}$  -0.01 mA) indicating that a reduction (Ag(I)/Ag(0)) is taking place and then the current rises to peak at  $E_{pa}$  -650 mV (with  $I_{pa}$  0.0035 mA) indicating oxidation process Ag(0)/Ag(I) but not of previously reduced species. This quasi-reversibility indicates that the species produced as a result of reduction of complex is unstable and it decomposes before the Ag(0)/Ag(I) oxidation. So the occurrence of oxidation may be attributed to Ag(0)/Ag(I) in different species instead of silver complex, i.e. silver complex decomposes during reduction and during oxidation merely decomposed species are oxidized (Figure 4).

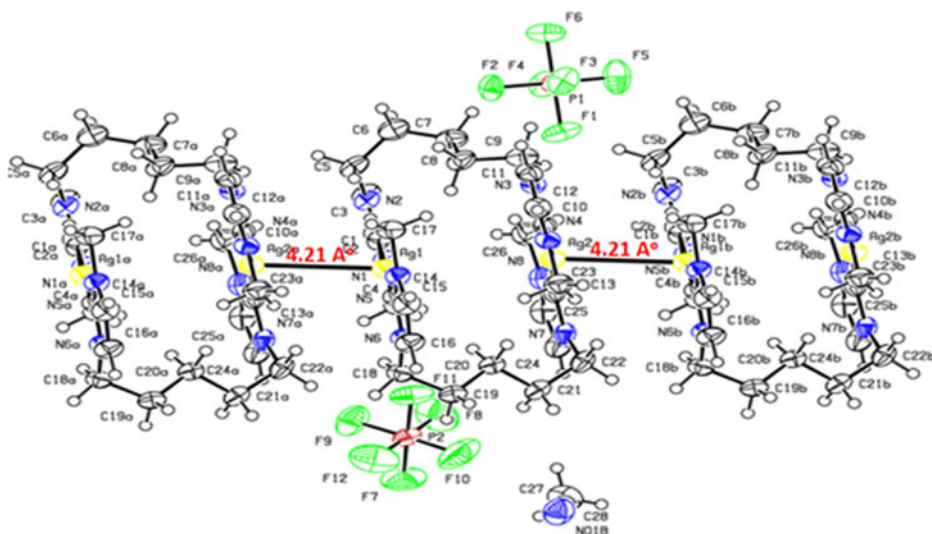


**Figure 1.** ORTEP view of **8** (50% probability level).

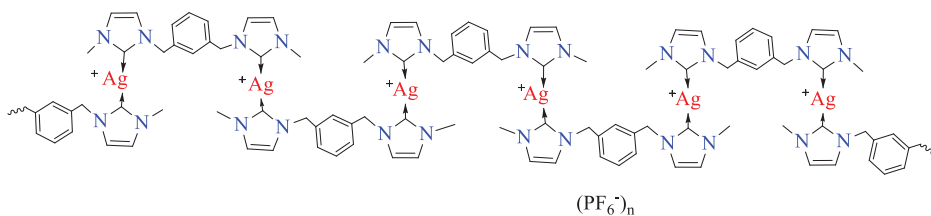
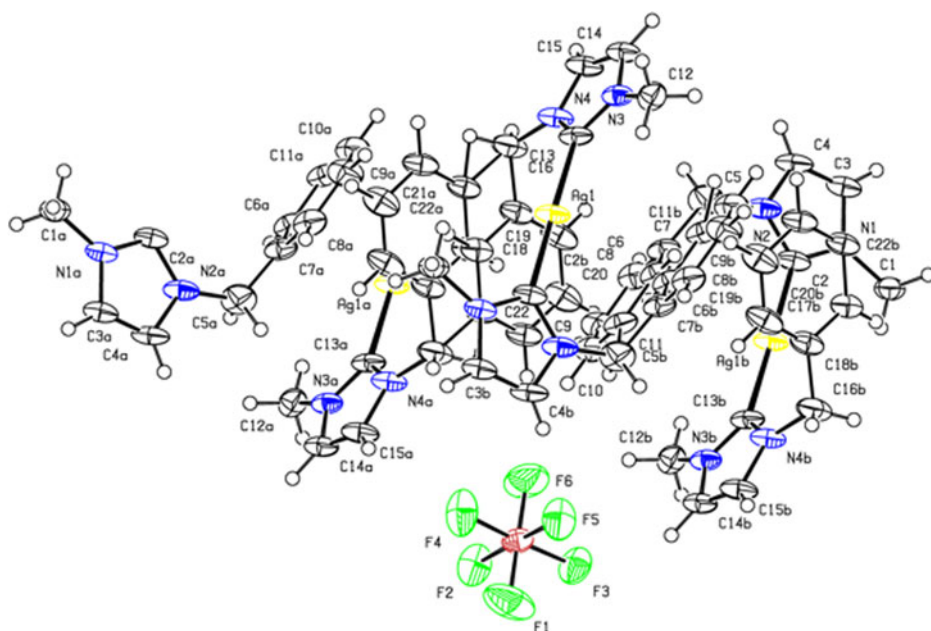


**Figure 2.** Polymeric structure of **9** revealed from X-ray crystallographic study.

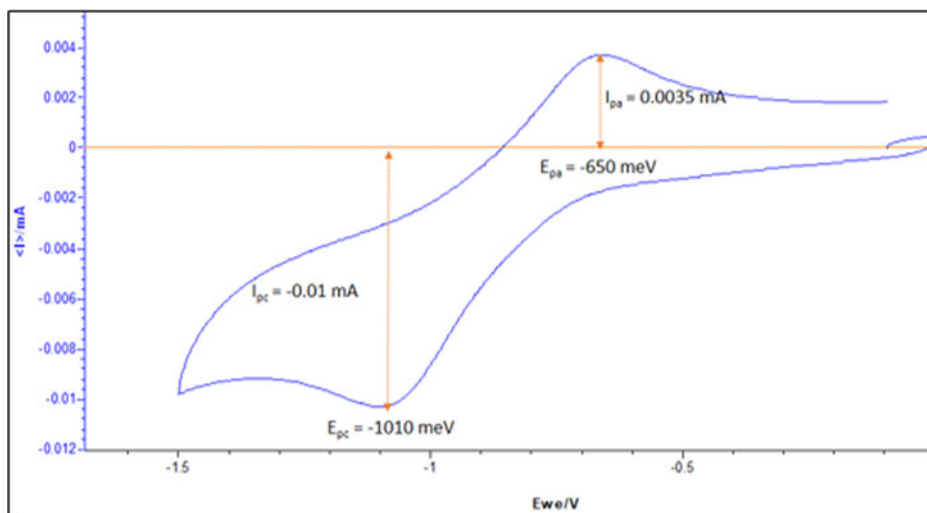
### 3.4. Anticancer activity

Several research groups have tested a number of NHC salts and Ag(I)–NHC complexes derived from imidazoles (with structural diversity) against various types of cancer cells [22, 37–39]. Herein, we report the cytotoxic activity of newly synthesized imidazolium-based compounds against breast cancer cell line (MDA-MB-231) and human colon cancer cell line (HCT-116) to study their antiproliferative potential.

IC<sub>50</sub> values of all NHC salts (**3–6**) and Ag(I)–NHC complexes (**7–10**) are given in Table 4. NHC salts exhibited lower cytotoxic activities against MDA-MB-231 and HCT-116 cells (with IC<sub>50</sub> values in the range of 60.24–155.30 μM) as compared to Ag(I)–NHC complexes (**7–10**) which showed pronounced cytotoxic activities (with IC<sub>50</sub> values ranging from 4.41 to 15.45 μM). It is also evident from the IC<sub>50</sub> values that the complexes are more cytotoxic to MDA-MB-231 cells while NHC salts are more cytotoxic to HCT-116 cells but almost non-toxic to MDA-MB-231 cells (very high IC<sub>50</sub> values). Reduced activities of salts compared to respective silver complexes can be attributed to silver–ligand coordination, resulting in increased antiproliferative characteristic of complexes due to involvement of silver ions in the cancer cell death mechanism. On the other hand, lower cytotoxic activities of these imidazole-based complexes compared to that of reported benzimidazole-based compounds [2, 13] is due to lack of benzene ring (as benzene ring increases the lipophilic feature and facilitates the



**Figure 3.** ORTEP view of crystal of **9** (50% probability level). The crystal structure reveals the polymeric nature of compound.

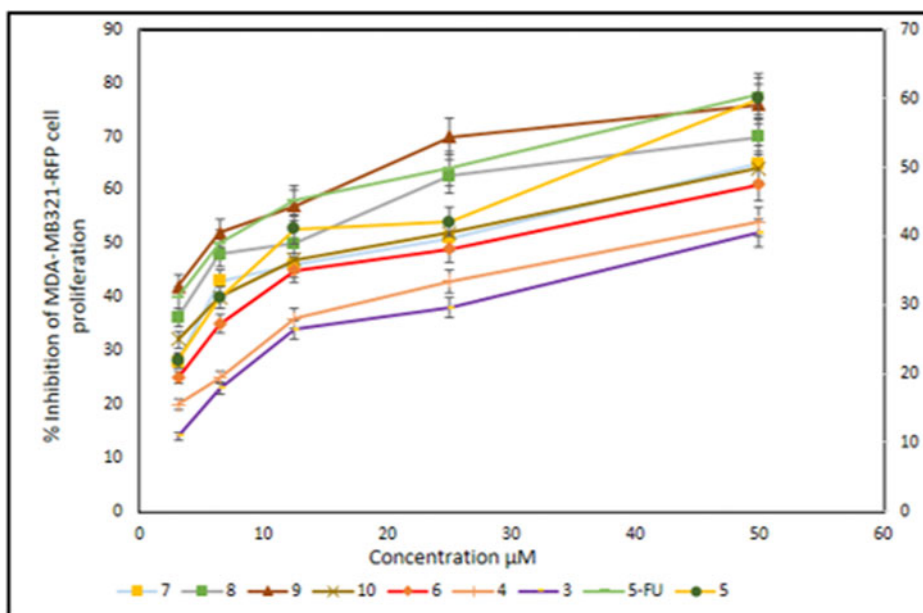


**Figure 4.** Cyclic voltammogram of **8** indicating the redox events. The measurements were carried out at 298 K on acetonitrile solutions containing a concentration of 0.1 M of  $[\text{Bu}_4\text{N}] [\text{PF}_6]$  and 1 mM sample.

passage of compound through cell membranes). It is also evident from  $\text{IC}_{50}$  values that aryl group as a linker decreases the cytotoxicity of ligands (**5** and **6**) ( $\text{IC}_{50}$  126.14, 79.48  $\mu\text{M}$  and 135.67, 60.24  $\mu\text{M}$ , respectively, against both cell lines) while increases that of silver complexes (**9** and **10**) ( $\text{IC}_{50}$  4.41, 7.82  $\mu\text{M}$  and 7.91–10.34  $\mu\text{M}$ , respectively, against both cell lines), which is attributed to enhanced lipophilicity that facilitates the smooth passage of  $\text{Ag}^+$  ions from cell membrane into the cell where they interrupt

**Table 4.** IC<sub>50</sub> (μM) values of NHC-ligands (3–6) and respective silver complexes (7–10) against MDA-MB-231 and HCT-116 cell lines.

Compounds (ligands)	IC <sub>50</sub> (μM)		Compounds (complexes)	IC <sub>50</sub> (μM)	
	MDA-MB-231	HCT-116		MDA-MB-231	HCT-116
Control (5FU)	7.50 ± 1.1	5.5 ± 0.8	Control (5FU)	7.50 ± 0.1	5.5 ± 0.3
3	155.32 ± 1.3	102.34 ± 1.1	7	8.23 ± 0.2	17.45 ± 1.6
4	152.12 ± 1.4	80.45 ± 1.4	8	7.42 ± 0.1	8.35 ± 1.2
5	126.14 ± 0.9	135.67 ± 1	9	4.41 ± 0.2	7.91 ± 1.1
6	79.48 ± 0.7	60.24 ± 0.8	10	7.82 ± 0.1	10.34 ± 0.4

**Figure 5.** Dose-dependent antiproliferative effect of synthesized ligands (3–6) and Ag(I)-NHC complexes (7–10) on MDA-MB-231 cells.

the cellular metabolic functionalities. Compound **9** showed enhanced activity (IC<sub>50</sub> 4.41 and 7.91 μM) against MDA-MB-231 and HCT-116 cells, respectively, due to its polymeric nature (as discussed in XRD section) which may be ascribed to the presence of more than two silver centers. Thus, the presence of imidazole moiety (instead of benzimidazole) decreases the biopotency, while longer side chains, presence of aryl linker as well as greater number of silver centers enhance the biopotency of imidazole-based Ag(I)-NHC complexes. Figures 5 and 6 depict dose-dependent cytotoxic effect of ligands and **3–10** against both cancer cell lines. It was observed that all compounds showed dose-dependent cytotoxic activities.

### 3.5. Anticancer mechanism of action and structure–activity relationship (SAR)

The mechanistic study during anticancer activity of NHC ligands and silver complexes has revealed that silver–ligand bonding results in increased biopotential by hindering quick release of Ag<sup>+</sup> ions into biological system [38, 40]. Gradual release of Ag<sup>+</sup> ions

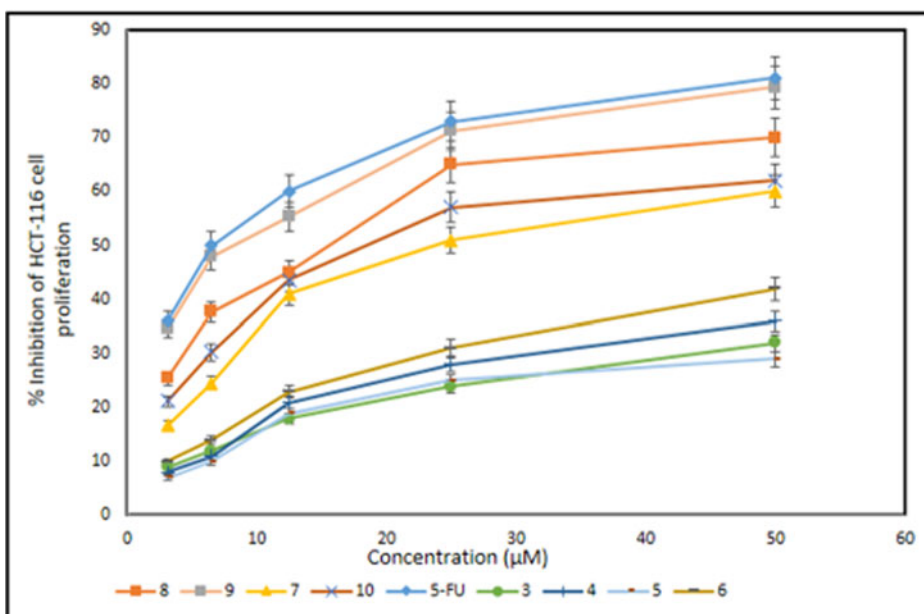


**Figure 6.** Dose-dependent antiproliferative effect of synthesized ligands (3–6) and Ag(I)–NHC complexes (7–10) on HCT-116 cells.

may be ascribed to the weak  $\pi$ -acceptor and strong  $\sigma$ -donor nature of Ag(I)–NHC complexes [38, 40]. Our previous studies [2, 26] have demonstrated that anticancer phenomenon mostly occurs through apoptotic pathway [8, 13, 26]. It has been established that lipophilic character depends on the chain length that facilitates the silver(I)–NHC compounds to penetrate the cell membranes, where they release silver ions which interact with cellular organelles and affect their functionalities [13, 41, 42]. Thus, ionization, delivery approaches and solubility of the silver sources are main parameters which control the interaction of silver with biological systems [41]. Hence, concluding the discussion, it may be generalized that longer side chains, presence of aryl linker as well as greater number of silver centers enhance the biopotency of Ag(I)–NHC complexes.

#### 4. Conclusion

A new series of dinuclear *N*-heterocyclic carbene-based ligands and silver complexes were synthesized. An interesting complex with polymeric structure (quite different from reported structures) was afforded as revealed from solid-state structure. The quasi-reversibility of redox events in electrochemical study of synthesized complexes indicated that reduction event produces unstable decomposed species and oxidation event may be ascribed to decomposed species. All ligands and complexes were studied for their *in vitro* antiproliferative potential against human breast cancer and colon cancer cells. Silver complexes were observed comparatively more cytotoxic than ligands. It was observed that breast cancer cells (MDA-MB-231) are more sensitive to complexes than colon cancer cells (HCT-116) while reverse is the case for NHC salts.

Increased chain length of NHC salts decreases its cytotoxicity while increases that of respective complexes. Hence, the presence of aryl linker, increased chain length, as well as multiple silver centers increase the anticancer potential of Ag(I)–NHC complexes. Further preclinical trials of synthesized drugs are under process.

### Additional information

Crystallographic data of the structures have been deposited with the Cambridge Crystallographic Data Center, CCDC 1890743 for **8** and CCDC 1890744 for **9**. This data can be obtained free of charge from CCDC via [www.ccdc.cam.ac.uk/data\\_request/cif](http://www.ccdc.cam.ac.uk/data_request/cif).

### Acknowledgement

The authors are obliged to Prof. Davit Zargarian for his assistance during IRSIP at Chemistry Department, University de Montreal, and to Dr. Loic Mangin for solving crystal structures and furnishing useful guidance to write this manuscript.

### Funding

The authors are grateful to Higher Education Commission (HEC), Pakistan for funding during IRSIP Vide Letter No. 1-8/HEC/HRD/2017/6940 and for the National Research Program for Universities Vide Letter No. 8396/Punjab/R&D/HEC/2017.

### Disclosure statement

No potential conflict of interest was reported by the authors.

### References

- [1] S.Y. Hussaini, R.A. Haque, M.R. Razali. *J. Organomet. Chem.*, **882**, 96 (2019).
- [2] A. Habib, M.N. Vishkaei, M.A. Iqbal, H.N. Bhatti, M.K. Ahmed, A.A. Majid. *J. Saudi Chem. Soc.*, in press. doi:10.1016/j.jscs.2019.03.002
- [3] A. Habib, M.A. Iqbal, H.N. Bhatti, M. Shahid. *Transition Met. Chem.*, **1** (2019). doi: 10.1007/s11243-019-00321-7
- [4] M.M. Gan, J.Q. Liu, L. Zhang, Y.Y. Wang, F.E. Hahn, Y.F. Han. *Chem. Rev.*, **118**, 9587 (2018).
- [5] C. Segarra, G. Guisado-Barrios, F.E. Hahn, E. Peris. *Organometallics*, **33**, 5077 (2014).
- [6] T. Fatima, R.A. Haque, M.R. Razali. *J. Mol. Struct.*, **1141**, 346 (2017).
- [7] Y.S. Wang, T. Feng, Y.Y. Wang, F.E. Hahn, Y.F. Han. *Angew. Chem. Int. Ed. Engl.* **57**, 15767 (2018).
- [8] R.A. Haque, M.A. Iqbal, S. Budagumpi, M.B. Khadeer Ahamed, A.M.A. Majid, N. Hasanudin. *Appl. Organomet. Chem.*, **27**, 214 (2013).
- [9] M. Rubio, M.A. Siegler, A.L. Spek, J.N. Reek. *Dalton Trans.*, **39**, 5432 (2010).
- [10] J.L. Yu, L. May, V. Lhotak, S. Shahrzad, S. Shirasawa, J.I. Weitz, B.L. Coomber, N. Mackman, J.W. Rak. *Blood*, **105**, 1734 (2005).
- [11] F. Bray, J. Ferlay, I. Soerjomataram, R.L. Siegel, L.A. Torre, A. Jemal. *CA Cancer J. Clin.*, **68**, 394 (2018).
- [12] H.K. Chan, S. Ismail. *Asian Pac. J. Cancer Prev.*, **15**, 5305 (2014).
- [13] M.A. Iqbal, R.A. Haque, M.B.K. Ahamed, A.A. Majid, S.S. Al-Rawi. *Med. Chem. Res.*, **22**, 2455 (2013).

- [14] J.A. Eremina, E.V. Lider, D.G. Samsonenko, L.A. Sheludyakova, A.S. Berezin, L.S. Klyushova, V.A. Ostrovskii, R.E. Trifonov. *Inorg. Chim. Acta*, **487**, 138 (2019).
- [15] S. Dhawan, N. Kerru, P. Awolade, A. Singh-Pillay, S.T. Saha, M. Kaur, S.B. Jonnalagadda, P. Singh. *Bioorg. Med. Chem.*, **26**, 5612 (2018).
- [16] A. Macháľková, L. Melounková, J. Vinklárek, I. Císařová, J. Honzčíek. *Inorg. Chim. Acta*, **485**, 125 (2019).
- [17] J. Wiemann, L. Fischer, M. Rohmer, R. Csuk. *Eur. J. Med. Chem.*, **156**, 861 (2018).
- [18] J.Q. Wang, X. Wang, Y. Wang, W.J. Tang, J.B. Shi, X.H. Liu. *Eur. J. Med. Chem.*, **156**, 493 (2018).
- [19] J.S. Yoon, D.B. Jarhad, G. Kim, A. Nayak, L.X. Zhao, J. Yu, H.-R. Kim, J.Y. Lee, V.A. Mulamootil, G. Chandra, W.S. Byun, S.K. Lee, Y.C. Kim, L.S. Jeong. *Eur. J. Med. Chem.*, **155**, 406 (2018).
- [20] N.N. Gibadullina, D.R. Latypova, V.A. Vakhitov, D.V. Khasanova, L.F. Zainullina, Y.V. Vakhitova, A.N. Lobov, B.I. Ugrak, Y.V. Tomilov, V.A. Dokichev. *J. Fluorine Chem.*, **211**, 94 (2018).
- [21] C.J. Yang, Z.L. Song, M. Goto, P.L. Hsu, X.S. Zhang, Q.R. Yang, Y.Q. Liu, M.J. Wang, S.L. Morris-Natschke, X.F. Shang. *Bioorg. Med. Chem. Lett.*, **27**, 4694 (2017).
- [22] M.A. Iqbal, M.I. Umar, R.A. Haque, M.B.K. Ahamed, M.Z.B. Asmawi, A.M.S.A. Majid. *J. Inorg. Biochem.*, **146**, 1 (2015).
- [23] R.A. Haque, N. Hasanudin, M.A. Hussein, S.A. Ahamed, M.A. Iqbal. *Inorg. Nano-Met. Chem.*, **47**, 131 (2017).
- [24] P.N. Shah, L.Y. Lin, J.A. Smolen, J.A. Tagaev, S.P. Gunsten, D.S. Han, G.S. Heo, Y. Li, F. Zhang, S. Zhang. *ACS Nano*, **7**, 4977 (2013).
- [25] R.A. Haque, P.O. Asekunowo, M.R. Razali. *Transition Met. Chem.*, **39**, 281 (2014).
- [26] M. Asif, M.A. Iqbal, M.A. Hussein, C.E. Oon, R.A. Haque, M.B.K. Ahamed, A.S.A. Majid, A.M.S.A. Majid. *Eur. J. Med. Chem.*, **108**, 177 (2016).
- [27] R. Gümüřada, M.E. Günay, N. Özdemir, B. Çetinkaya. *J. Coord. Chem.*, **69**, 1463 (2016).
- [28] C.V. Maftei, E. Fodor, P.G. Jones, M. Freytag, M.H. Franz, G. Kelter, H.-H. Fiebig, M. Tamm, I. Neda. *Eur. J. Med. Chem.*, **101**, 431 (2015).
- [29] M. Kalođlu, N. Kalođlu, İ. Özdemir, S. Günal, İ. Özdemir. *Bioorg. Med. Chem.*, **24**, 3649 (2016).
- [30] J.C. Garrison, W.J. Youngs. *Chem. Rev.*, **105**, 3978 (2005).
- [31] M.O. Karatař, B. Olgundeniz, S. Günal, İ. Özdemir, B. Alicı, E. Çetinkaya. *Bioorg. Med. Chem.*, **24**, 643 (2016).
- [32] Y.B. Dong, J.P. Ma, R.Q. Huang, M.D. Smith, H.C. zur Loye. *Inorg. Chem.*, **42**, 294 (2003).
- [33] P.L. Chiu, C.Y. Chen, J.Y. Zeng, C.Y. Lu, H.M. Lee. *J. Organomet. Chem.*, **690**, 1682 (2005).
- [34] V.J. Catalano, M.A. Malwitz. *Inorg. Chem.*, **42**, 5483 (2003).
- [35] V.J. Catalano, A.L. Moore. *Inorg. Chem.*, **44**, 6558 (2005).
- [36] H.Z. Kaplan, B. Li, J.A. Byers. *Organometallics*, **31**, 7343 (2012).
- [37] A. Gautier, F. Cisnetti. *Metallomics*, **4**, 23 (2012).
- [38] W. Liu, R. Gust. *Chem. Soc. Rev.*, **42**, 755 (2013).
- [39] L. Oehninger, R. Rubbiani, I. Ott. *Dalton Trans.*, **42**, 3269 (2013).
- [40] C.G. Hartinger, M.A. Jakupec, S. Zorbas-Seifried, M. Groessl, A. Egger, W. Berger, H. Zorbas, P.J. Dyson, B.K. Keppler. *Chem. Biodivers.*, **5**, 2140 (2008).
- [41] A. Kascatan-Nebioglu, M.J. Panzner, C.A. Tessier, C.L. Cannon, W.J. Youngs. *Coord. Chem. Rev.*, **251**, 884 (2007).
- [42] E.C. Friedberg, G.C. Walker, W. Siede, R.D. Wood, *DNA Repair and Mutagenesis*. American Society for Microbiology Press, Washington, USA (2005).